ELSEVIER

Biophysical Chemistry 111 (2004) 247–257

Biophysical Chemistry

www.elsevier.com/locate/bpc

Absorption and fluorescence spectra of ring-substituted indole-3-acetic acids

Dejana Carić[a], Vladislav Tomišić[b], Marina Kveder[c], Nives Galić[b], Greta Pifat[c], Volker Magnus[c,*], Milan Šoškić[a]

[a] *Faculty of Agronomy, Svetošimunska cesta 25, 10000 Zagreb, Croatia*
[b] *Department of Chemistry, Faculty of Science, Marulićev trg 19, P.O. Box 163, 10001 Zagreb, Croatia*
[c] *Ruđer Bošković Institute, Bijenička cesta 54, P.O. Box 180, 10002 Zagreb, Croatia*

Received 20 April 2004; received in revised form 2 June 2004; accepted 3 June 2004
Available online 7 July 2004

Abstract

The absorption and fluorescence spectra of indole-3-acetic acid (**1**), a plant growth regulator (auxin) and experimental cancer therapeutic, 29 ring-substituted derivatives and the 7-aza analogue (1*H*-pyrrolo[2,3*b*]pyridine-3-acetic acid) are compared. Two to four absorbance maxima in the 260–310-nm range are interpreted as overlapping vibronic lines of the $^1L_a \leftarrow {}^1A$ and $^1L_b \leftarrow {}^1A$ transitions. Two further maxima in the 200–230-nm region are assigned to the $^1B_a \leftarrow {}^1A$ and $^1B_b \leftarrow {}^1A$ transitions. 4- and 7-Fluoroindole-3-acetic acid exhibit blue shifts with respect to **1**, most other derivatives show red shifts. All indole-3-acetic acids studied, with the exception of chloro-, bromo- and 4- or 7-fluoro-derivatives, fluoresce at 345–370 nm when excited at 275–280 nm. 7-Azaindole-3-acetic acid emits at 411 nm. The fluorescence quantum yield of 6-fluoroindole-3-acetic acid significantly exceeds that of **1** (0.3); the other derivatives have lower quantum yields. The plant-growth promoting activity of the ring-substituted indole-3-acetic acids studied correlates with the position of the $^1B_b \leftarrow {}^1A$ transition band.

Keywords: Auxin; Ring-substituted indole-3-acetic acid; UV absorbance; Fluorescence; Structure–activity relationship

1. Introduction

The endogenous 'auxin', indole-3-acetic acid (IAA, **1**, Fig. 1), the first phytohormone ever discovered, is now known to coordinate plant growth and development from the seedling stage to fruit ripening and senescence [1]. In a search for synthetic analogues more suitable for manipulating growth and morphogenesis in crop plants and ornamentals, a large number of ring-substituted indole-3-acetic acids were prepared, in addition to a myriad of non-indolic auxins [2]. Some of the former were later found as natural compounds: **8** as a regulator of fruit development in peas [3–5] and **24** as a metabolite of soil bacteria [6,7]. In humans and mammals, **1** is a minor tryptophan metabolite with no obvious role in the healthy organism, but a factor of concern in liver and kidney disease [8–10]. Its ring-methoxylated and-hydroxylated derivatives **15** and **16** are important breakdown products of biogenic amines, such as the neurotransmitter, serotonin, the hormone, melatonin and structurally related drugs. Other ring-substituted derivatives, originally developed as plant growth regulators, are now receiving attention as promising candidates for cancer therapeutics [11–13].

Understanding the roles of auxins in human, animal and plant systems requires answers to questions such as (1) What are their levels at the sites of action? (2) How do they interact with response-mediating proteins? (3) How are molecular structure and biological activity correlated? Spectroscopic and fluorimetric techniques can provide answers to all three questions permitting, for instance, fast and sensitive monitoring of the levels of ring-substituted indole-3-acetic acids in body fluids, and of their interactions with response-mediating proteins, as long as the target compounds can be reliably distinguished from endogenous indoles (including the tryptophan moieties in proteins). The literature data covering the respective absorbance and fluorescence properties are, however, incomplete, scattered

* Corresponding author. Tel.: +385-1-4561-143; fax: +385-1-4561-177.
E-mail address: magnus@irb.hr (V. Magnus).

0301-4622/$ - see front matter © 2004 Elsevier B.V. All rights reserved.
doi:10.1016/j.bpc.2004.06.006

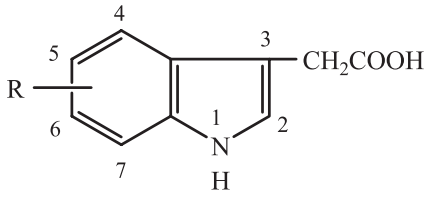

Compound	R	Compound	R
1	H	**16**	5-OH
2	2-CH_3	**17**	5-$OCH_2C_6H_5$
3	2-C_2H_5	**18**	6-CH_3
4	2-*n*-C_3H_7	**19**	6-C_2H_5
5	4-CH_3	**20**	6-F
6	4-C_2H_5	**21**	6-Cl
7	4-F	**22**	7-CH_3
8	4-Cl	**23**	7-F
9	5-CH_3	**24**	7-Cl
10	5-C_2H_5	**25**	4,6-Cl_2
11	5-*n*-C_3H_7	**26**	5,6-Cl_2
12	5-*n*-C_4H_9	**27**	5,7-Cl_2
13	5-F	**28**	6,7-Cl_2
14	5-Br	**29**	4,7-Cl_2
15	5-OCH_3	**30**	4,5-Cl_2

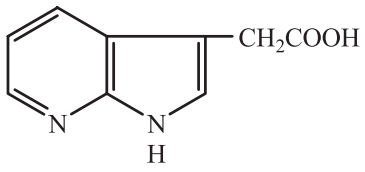

31

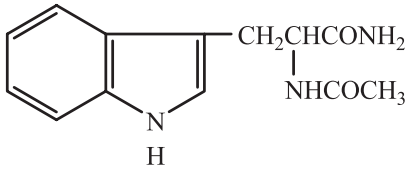

32

Fig. 1. Structural formulae of the compounds studied.

through a bewildering number of papers, and not strictly comparable because they were obtained on instruments differing in design and level of sophistication. This prompted us to collect absorbance and fluorescence data for **1**, its 7-aza-analogue **31** and 29 of its ring-substituted derivatives (**2**–**30**) (Fig. 1), with focus on alkylated and halogenated auxins. In spite of many similarities, we observed a number of specific features which may be exploited in biochemical analysis. The red shift in the absorbance maxima of dichlorinated indole-3-acetic acids **25**–**30**, and in the fluorescence of aza-analogue **31**, should, for instance, be sufficient to permit quantification in (suitably prepurified) extracts of biomedical material which contain endogenous **1**. Another probe worth testing in auxin-protein binding studies would be ring-fluorinated derivative **20**, for which we find a fluorescence quantum yield of 0.53 (at pH 7.2) which significantly exceeds that of **1** (0.33) as well as that of free and polypeptide-bound tryptophan (0.02–0.35) [14]. In addition to those analytical aspects, comparison of the positions of the UV absorbance maxima in the set of ring-substituted indole-3-acetic acids examined herein reveals a correlation with plant-growth promoting activity, one of the biological effects exhibited by auxins.

2. Experimental

2.1. Materials

The solution of rhodamine 101 in ethylene glycol, used for the correction of excitation intensities in fluorescence spectroscopy, was supplied by Varian (cat. no. 66 100217 00). The *N*-acetyl-L-tryptophanamide (NATA, **32**), utilized as a standard in fluorescence quantum yield measurements, was from Fluka (Buchs, Switzerland).

The auxins, **1**, **2**, **13**, **14** and **15**–**17**, were purchased from commercial suppliers. 1*H*-Pyrrolo[2,3*b*]pyridine-3-acetic acid (7-azaindole-3-acetic acid, **31**) was synthesized after Robison and Robison [15,16]. Dichlorinated auxins **25**–**30** were donated by Dr. K.C. Engvild or prepared according to

his procedures [17]. The latter afforded **26** and **30** as an equimolar mixture, which was separated by preparative HPLC [18]. The remaining ring-halogenated indole-3-acetic acids were synthesized as outlined by Reinecke et al. [19]. The methods used for the preparation of ring-alkylated indole-3-acetic acids were summarized by Nigović et al. [20] and Antolić et al. [21].

Stock solutions of **1** and its derivatives were prepared in spectrophotometric grade 95% ethanol (Fluka). The buffers used for measurements at controlled pH contained, per liter, 40 mmol boric acid, 37.5 mmol orthophosphoric acid, 40 mmol acetic acid and the volume of 200 mM sodium hydroxide solution required to reach the desired pH. For pH ≈ 0, the buffer was replaced by 1 M HCl; 1 M NaOH was used for pH ≈ 14. pH values were measured using a Radiometer (Copenhagen, Denmark) pH Meter 26 equipped with a Radiometer GK 2401 B combined (Ag/AgCl+glass) electrode. The electrode was calibrated with standard buffers (Kemika, Zagreb, Croatia).

2.2. UV spectroscopy

UV absorption spectra were recorded, against the solvent, at (25 ± 0.1) °C, using a Varian Cary 5 spectrophotometer operated in double-beam mode. The wavelength range covered was 200–350 nm. Quartz cells of 1-cm path length were used throughout and absorbances were sampled at 0.1-nm intervals. Samples were prepared by diluting the respective stock solutions (in 95% ethanol) with 95% ethanol or the appropriate aqueous buffer, to a concentration of 40–80 μmol dm^{-3}. The ethanol concentrations in aqueous samples (buffer solutions) were, in most cases, 3% (v/v) or less, and 5% (v/v) for **26**, **27** and **30** which were available in limited quantities (less concentrated stock solutions).

2.3. Steady-state fluorescence spectroscopy

Fluorescence measurements were carried out on a Varian Cary Eclipse fluorescence spectrophotometer at 25 °C using 1-cm path quartz cells. The bandwidths of the excitation and emission monochromators were 2.5 and 5 nm, respectively, with a data-sampling interval of 0.5 nm. Excitation maxima were determined from excitation spectra covering the range of 200–350 nm. Emission spectra were recorded from 300 to 500 nm and corrected for the effects of time- and wavelength-dependent light-source fluctuations using a standard of rhodamine 101, a diffuser provided with the fluorimeter and the software supplied with the instrument.

For fluorescence measurements at pH 2–12, the stock solutions (in 95% ethanol) were diluted with the buffer specified above. The final ethanol concentration in the solutions used for fluorescence measurements was less than 0.5% (v/v). The final sample concentrations were ca. 5 μmol dm^{-3} to achieve an optical absorbance below 0.05, at the excitation wavelength.

Relative fluorescence quantum yields were determined according to Miller [22] using Eq. (1):

$$Q_x = Q_s \frac{A_s D_x n_x^2}{A_x D_s n_s^2} \quad (1)$$

wherein Q is the emission quantum yield, A is the absorbance at the excitation wavelength, D is the area under the corrected emission curve and n is the refractive index of the solvents used. The subscripts s and x refer to the standard and to the unknown, respectively. The standard we used was *N*-acetyl-L-tryptophanamide (**32**) with a published fluorescence quantum yield of 0.14 [23,24]. All samples were purged with argon to displace oxygen. The reproducibility (difference between the largest and the smallest value in a series of five independent measurements, divided by their arithmetic mean) of quantum yield measurements was better than 10%.

3. Results and discussion

3.1. UV absorption spectroscopy

The absorbance data for **1**, ring-substituted derivatives **2**–**30**, aza-analogue **31** and *N*-acetyl-L-tryptophanamide (**32**), measured in ethanol (95%) solution and in aqueous buffer, pH 7.2, are presented in Table 1. Up to seven absorbance maxima or shoulders are observed, up to five of which occur in the 250–330-nm region. Their positions and relative intensities represent a fingerprint characterizing each individual compound (Fig. 2). A sharper, more intense, maximum occurs at 216–232 nm. A further maximum at 200–208 nm was consistently observed in ethanol solutions of **1** and 27 of its derivatives, but is at the very edge of the spectral range recommended for ethanol as a solvent [25], which may impact on the accuracy of the respective values for λ_{max} and ε given in Table 1. This maximum cannot be

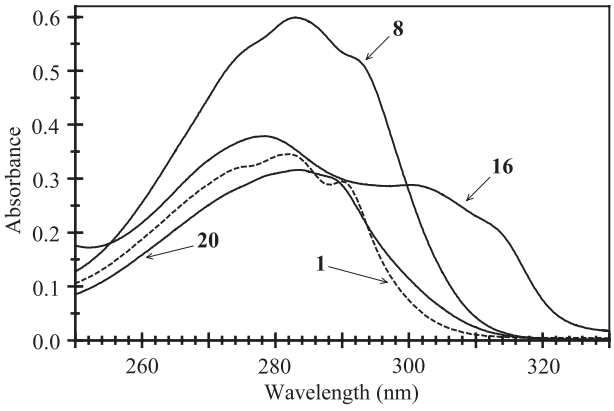

Fig. 2. Fingerprint region of the UV absorbance spectra (in 95% ethanol) of **1** ($c = 6.032 \times 10^{-5}$ mol dm^{-3}), **8** ($c = 1.003 \times 10^{-4}$ mol dm^{-3}), **16** ($c = 7.027 \times 10^{-5}$ mol dm^{-3}) and **20** ($c = 5.746 \times 10^{-5}$ mol dm^{-3}); optical path = 1 cm.

Table 1
Absorbance maxima [ranked from 1 to 7, in ascending (by wavelength) order] of indole-3-acetic acid (**1**), its ring-substituted derivatives **2**–**30**, 7-azaindole-3-acetic acid (**31**) and *N*-acetyl-L-tryptophanamide (NATA, **32**) in solvents A (95% ethanol) and B (aqueous buffer, pH 7.2)

Compound	Solvent	λ_{max} (nm) [log ε (mol^{-1} dm^3 cm^{-1})]						
		1[a]	2	3	4	5	6	7
1	A	201.1 [4.26]	222.7 [4.50]	n.d.[b]	276.3[c] [3.73]	n.d.[b]	282.0 [3.76]	290.0 [3.69]
	B	n.d.[b]	220.7 [4.49]	n.d.[b]	275.0[c] [3.70]	n.d.[b]	280.0 [3.72]	287.6[c] [3.66]
2	A	202.4 [4.23]	225.8 [4.44]	n.d.[b]	276.1[c] [3.77]	n.d.[b]	282.3 [3.80]	289.8 [3.73]
	B	n.d.[b]	222.9 [4.39]	n.d.[b]	271.8 [3.76]	n.d.[b]	278.8[c] [3.74]	287.7[c] [3.69]
3	A	201.2 [4.25]	226.5 [4.47]	n.d.[b]	276.2[c] [3.81]	n.d.[b]	283.1 [3.85]	290.4 [3.80]
	B	n.d.[b]	224.6 [4.48]	n.d.[b]	275.9[c] [3.82]	n.d.[b]	281.1 [3.84]	288.4[c] [3.79]
4	A	201.5 [4.28]	226.4 [4.49]	n.d.[b]	276.5[c] [3.84]	n.d.[b]	283.1 [3.88]	290.4 [3.82]
	B	n.d.[b]	225.1 [4.49]	n.d.[b]	n.r.[d]	n.d.[b]	281.5 [3.86]	288.4[c] [3.80]
5	A	201.4 [4.25]	224.7 [4.50]	n.d.[b]	275.9 [3.75]	n.d.[b]	281.0 [3.75]	291.4[c] [3.64]
	B	n.d.[b]	222.4 [4.49]	n.d.[b]	274.2 [3.70]	n.d.[b]	279.1 [3.70]	289.9[c] [3.60]
6	A	202.7 [4.27]	223.7 [4.52]	n.d.[b]	276.3[c] [3.80]	n.d.[b]	281.3 [3.81]	291.3 [3.71]
	B	n.d.[b]	222.2 [4.26]	n.d.[b]	275.3[c] [3.51]	n.d.[b]	280.0 [3.52]	290.6[c] [3.42]
7	A	n.r.[d]	220.6 [4.65]	267.8 [3.73]	275.0[c] [3.70]	n.d.[b]	n.d.[b]	286.6[c] [3.53]
	B	n.d.[b]	218.6 [4.62]	266.3 [3.71]	274.1[c] [3.67]	n.d.[b]	n.d.[b]	285.5[c] [3.50]
8	A	201.0 [4.31]	225.9 [4.55]	n.d.[b]	277.3[c] [3.77]	n.d.[b]	283.4 [3.80]	291.1[c] [3.75]
	B	n.d.[b]	224.4 [4.56]	n.d.[b]	276.6[c] [3.77]	n.d.[b]	281.9 [3.80]	290.7[c] [3.74]
9	A	203.4 [4.31]	224.6 [4.47]	n.d.[b]	279.4 [3.75]	n.d.[b]	286.2 [3.75]	296.2[c] [3.62]
	B	n.d.[b]	222.9 [4.41]	n.d.[b]	279.1 [3.67]	n.d.[b]	285.4 [3.68]	295.2[c] [3.57]
10	A	203.4 [4.32]	225.1 [4.50]	n.d.[b]	279.5 [3.76]	n.d.[b]	285.8 [3.76]	295.5[c] [3.64]
	B	n.d.[b]	223.1 [4.48]	n.d.[b]	279.1 [3.72]	n.d.[b]	284.8 [3.72]	294.3[c] [3.62]
11	A	202.4 [4.32]	225.8 [4.50]	n.d.[b]	279.7 [3.75]	n.d.[b]	286.0 [3.75]	295.5[c] [3.63]
	B	n.d.[b]	223.3 [4.47]	n.d.[b]	278.9 [3.70]	n.d.[b]	285.0 [3.71]	294.4[c] [3.60]
12	A	202.2 [4.33]	225.7 [4.50]	n.d.[b]	279.7 [3.76]	n.d.[b]	286.0 [3.76]	295.8[c] [3.64]
	B	n.d.[b]	223.1 [4.48]	n.d.[b]	279.0 [3.71]	n.d.[b]	284.8 [3.72]	294.3[c] [3.61]
13	A	202.8 [4.22]	222.3 [4.37]	n.d.[b]	n.d.[b]	282.2[c] [3.81]	286.9 [3.81]	296.6[c] [3.70]
	B	n.d.[b]	220.2 [4.33]	n.d.[b]	n.d.[b]	280.2[c] [3.75]	285.1 [3.76]	293.0[c] [3.68]
14	A	200.1 [4.26]	229.0 [4.47]	n.d.[b]	284.3[c] [3.63]	n.d.[b]	290.6 [3.66]	298.3[c] [3.57]
	B	n.d.[b]	226.7 [4.50]	n.d.[b]	282.9[c] [3.67]	n.d.[b]	288.7 [3.69]	297.0[c] [3.61]
15	A	203.6 [4.36]	223.7 [4.37]	n.d.[b]	278.4 [3.78]	n.d.[b]	295.7[c] [3.69]	307.9[c] [3.53]
	B	n.d.[b]	222.0 [4.37]	n.d.[b]	277.7 [3.75]	n.d.[b]	291.6[c] [3.69]	302.8[c] [3.57]
16	A	203.5 [4.32]	222.6 [4.28]	n.d.[b]	278.2 [3.73]	n.d.[b]	300.3 [3.61]	310.7[c] [3.51]
	B	n.d.[b]	221.0 [4.31]	n.d.[b]	277.7 [3.75]	n.d.[b]	295.0[c] [3.68]	302.5[c] [3.59]
17[e]	A	202.2 [4.55]	222.9[c] [4.46]	n.d.[b]	279.1 [3.84]	n.d.[b]	296.2[c] [3.75]	308.3[c] [3.55]
	B	n.d.[b]	219.6[c] [4.47]	n.d.[b]	278.5 [3.79]	n.d.[b]	292.6[c] [3.73]	303.0[c] [3.59]
18	A	202.6 [4.28]	224.8 [4.56]	n.d.[b]	278.1[c] [3.75]	282.8 [3.77]	285.2[c] [3.76]	292.7 [3.70]
	B	n.d.[b]	222.8 [4.54]	n.d.[b]	276.5[c] [3.71]	281.1 [3.72]	n.r.[d]	290.4[c] [3.65]
19	A	201.9 [4.30]	225.5 [4.57]	n.d.[b]	277.7[c] [3.78]	282.4 [3.80]	284.7[c] [3.79]	292.3 [3.72]
	B	n.d.[b]	223.3 [4.51]	n.d.[b]	276.5[c] [3.70]	281.0 [3.71]	n.r.[d]	289.9[c] [3.64]
20	A	201.0 [4.26]	220.4 [4.49]	n.d.[b]	275.0[c] [3.70]	281.0[c] [3.73]	283.4 [3.74]	287.5 [3.72]
	B	n.d.[b]	218.2 [4.46]	n.d.[b]	n.d.[b]	279.1[c] [3.69]	281.9 [3.69]	285.6[c] [3.67]
21	A	201.5 [4.26]	228.5 [4.53]	n.d.[b]	280.2[c] [3.74]	n.d.[b]	286.4 [3.77]	294.6 [3.72]
	B	n.d.[b]	227.5 [4.49]	n.d.[b]	279.4[c] [3.67]	n.d.[b]	285.0 [3.69]	292.9[c] [3.63]
22	A	203.1[c] [4.29]	221.7 [4.57]	n.d.[b]	274.6 [3.80]	279.9 [3.81]	n.d.[b]	289.1[c] [3.71]
	B	n.d.[b]	219.9 [4.55]	n.d.[b]	274.0[c] [3.75]	278.9 [3.76]	n.d.[b]	288.4[c] [3.66]
23	A	n.d.[b]	218.3 [4.58]	267.7 [3.72]	275.7[c] [3.70]	n.d.[b]	279.4[c] [3.67]	288.1 [3.56]
	B	n.d.[b]	216.6 [4.55]	266.9 [3.68]	274.3[c] [3.65]	n.d.[b]	n.r.[d]	286.2 [3.51]
24	A	202.1 [4.33]	223.9 [4.55]	n.d.[b]	278.0[c] [3.75]	n.d.[b]	285.1 [3.78]	294.2 [3.71]
	B	n.d.[b]	222.4 [4.52]	n.d.[b]	276.5[c] [3.72]	n.d.[b]	283.8 [3.74]	292.1 [3.68]
25	A	200.6 [4.29]	232.4 [4.58]	n.d.[b]	281.5[c] [3.72]	n.d.[b]	288.0 [3.77]	294.5[c] [3.74]
	B	n.d.[b]	230.6 [4.57]	n.d.[b]	281.5[c] [3.75]	n.d.[b]	286.6 [3.78]	292.8[c] [3.74]
26	A	200.7 [4.35]	232.4 [4.54]	n.d.[b]	288.6[c] [3.71]	n.d.[b]	295.1 [3.76]	304.3 [3.72]
	B	n.d.[b]	231.0 [4.51]	n.d.[b]	286.8[c] [3.67]	n.d.[b]	293.5 [3.71]	302.8 [3.66]
27	A	205.3 [4.43]	230.8 [4.54]	n.d.[b]	287.0[c] [3.75]	n.d.[b]	294.1 [3.76]	304.1[c] [3.68]
	B	n.d.[b]	229.2 [4.48]	n.d.[b]	285.9[c] [3.69]	n.d.[b]	293.0 [3.71]	302.5[c] [3.63]
28	A	203.5 [4.32]	229.7 [4.53]	n.d.[b]	281.7[c] [3.76]	n.d.[b]	288.0 [3.81]	295.3[c] [3.77]
	B	n.d.[b]	227.3 [4.51]	n.d.[b]	280.8[c] [3.76]	n.d.[b]	286.8 [3.79]	294.4[c] [3.75]
29	A	208.0 [4.32]	228.4 [4.54]	n.d.[b]	283.1[c] [3.76]	n.d.[b]	290.6 [3.79]	298.2[c] [3.76]
	B	n.d.[b]	226.2 [4.56]	n.d.[b]	282.2[c] [3.80]	n.d.[b]	288.2 [3.82]	297.3 [3.77]
30	A	204.5 [4.33]	229.9 [4.54]	n.d.[b]	285.0[c] [3.75]	n.d.[b]	290.8 [3.77]	300.0[c] [3.70]
	B	n.d.[b]	228.0 [4.53]	n.d.[b]	283.0[c] [3.74]	n.d.[b]	289.0 [3.76]	299.0[c] [3.67]

Table 1 (*continued*)

Compound	Solvent	λ_{max} (nm) [log ε (mol^{-1} dm^3 cm^{-1})]						
		1[a]	2	3	4	5	6	7
31	A	n.d.[b]	225.3 [4.27]	n.d.[b]	n.d.[b]	n.d.[b]	290.6 [3.80]	296.0[c] [3.75]
	B	n.d.[b]	223.2 [4.25]	n.d.[b]	n.d.[b]	n.d.[b]	289.6 [3.79]	294.6[c] [3.75]
32	A	202.3 [4.33]	222.2 [4.56]	n.d.[b]	275.2[c] [3.77]	n.d.[b]	281.7 [3.80]	290.1 [3.73]
	B	n.d.[b]	220.0 [4.56]	n.d.[b]	273.5[c] [3.75]	n.d.[b]	279.6 [3.77]	287.9 [3.70]

[a] The batch of solvent A used in this work afforded quantitatively reproducible spectra down to 200 nm, but it should be noted that ethanol is usually not recommended for wavelengths below 204 nm [25], and the data shown for maximum 1 may not be quite as accurate as for maxima 2–7. Maximum 1 could not be recorded in solvent B, which was not sufficiently transparent at wavelengths below 210 nm.

[b] n.d. = not detected.

[c] Shoulder.

[d] n.r. = not resolved (very weak inflection; wavelength could not be accurately determined).

[e] An additional maximum attributable to the 5-benzyloxy moiety was observed at 215.8 nm [log ε = 4.49] in solvent A and at 217.1 nm [log ε = 4.48] in solvent B.

observed in aqueous buffer solutions, which are not sufficiently transparent at wavelengths below 210 nm. Otherwise, spectra in ethanol and buffer solutions show corresponding features, except for a very weak shoulder at 275 nm in the ethanol spectrum of **20** which cannot be observed in aqueous buffer. Generally, ethanol solutions afford better resolved spectra, frequently showing clear maxima where indistinct inflections occur in buffer solutions. In ethanol, corresponding spectral features occur at slightly higher wavelengths than in an aqueous environment. For maximum 2 (see Table 1 for definition), the difference is, in most cases, 1.5–2.5 nm, with no clear dependence on the ring substituent. For maximum 4, the difference is frequently smaller or none. For maxima 6 and 7, the shift can be as large as 8 nm if ring substituents are linked to the indole nucleus via oxygen (**15**–**17**).

UV absorbance in aqueous buffer may depend on its pH value. This issue was addressed for two model compounds: **1** and **31** which bears an additional dissociable group changing its degree of ionization in the physiological pH range. The positions of the absorbance maxima at pH 2–12 are listed in Table 2. The deprotonation of the carboxyl group of **1** (pK_a = 4.75 [26]), which is practically complete at pH 7, is reflected by a bathochromic shift largest for the lowest-wavelength (218.1 → 220.8 nm), and smallest for the highest-wavelength (287.3 → 287.5 nm) band which simultaneously transforms from a weak maximum into a flat shoulder. There are no further changes, when the pH is increased from 7 to 12. In **31**, both the carboxyl group (expected pK_a as for **1**) and N-7 ($pK_a \approx 4.5$ for 7-azaindole [27]) are deprotonated in about the same pH-range. The resulting spectral shifts are about the same as for **1**, but in the *opposite* direction (hypsochromic). Simultaneously, absorption intensity shifts from the high-wavelength to the low-wavelength band, and a weak shoulder appears at 295 ± 0.3 nm. The dissociation-induced changes in the overall appearance of the absorption spectra of **1** and **31** are shown in Fig. 3. In the pH range of 5–8, in which most physiological reactions occur, the positions of the absorbance bands for both model compounds change by maximally 1 nm and the corresponding ε values by maximally 2% for **1**, and maximally 9% for **31**. This may well be less than the usual experimental error in spectroscopic measurements in biological samples, which are rarely completely free of interfering materials.

The UV spectra of indole-3-acetic acids which do not contain additional dissociable ring-substituents should show the same kind of pH-dependence as the unsubstituted parent compound. The 5-hydroxy moiety of **16** has a pK_a value of 11.2 [28]. Thus, even with this substituent,

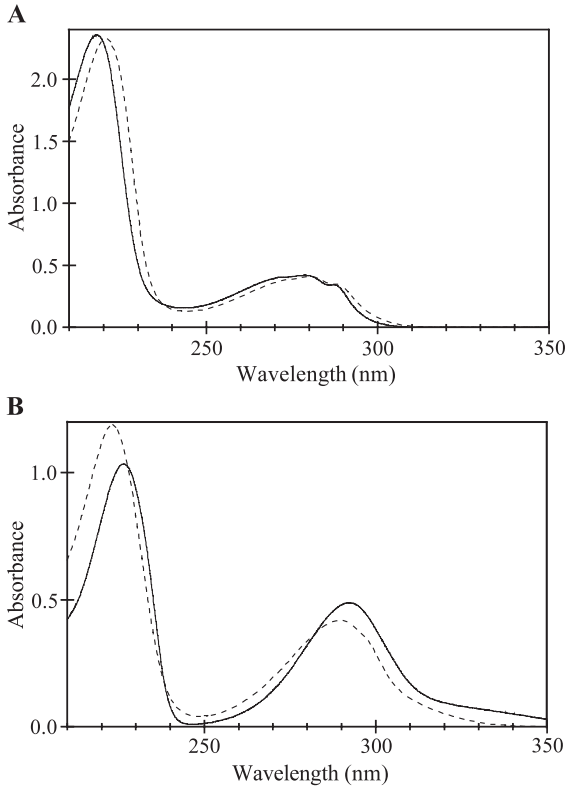

Fig. 3. UV spectra of (A) **1** ($c = 7.535 \times 10^{-5}$ mol dm^{-3}) and (B) **31** ($c = 6.507 \times 10^{-5}$ mol dm^{-3}) in their fully protonated forms (pH 2.0, full lines) and after deprotonation (pH 7.0, broken lines) at the carboxyl group and, for **31**, simultaneously at N-7.

Table 2
Absorbance maxima of indole-3-acetic (**1**) and 7-azaindole-3-acetic (**31**) acids in aqueous buffer (see Section 2.1 for composition) at different pH values

pH	**1**		**31**	
	λ_{max} (nm)	log ε (mol^{-1} dm^3 cm^{-1})	λ_{max} (nm)	log ε (mol^{-1} dm^3 cm^{-1})
2.0	218.1	4.50	226.4	4.20
	273.1[a]	3.73		
	278.7	3.75	292.2	3.88
	287.3	3.66		
4.0	218.4	4.48	225.8	4.19
	273.7[a]	3.71		
	278.9	3.73	292.0	3.85
	287.2	3.65		
5.0	220.2	4.48	224.1	4.23
	274.4[a]	3.71		
	279.7	3.73	291.1	3.83
	287.3[a]	3.66		
6.0	220.8	4.49	223.3	4.25
	274.4[a]	3.71		
	280.2	3.74	290.1	3.80
	287.5[a]	3.67	295.0[a]	3.76
7.0	220.8	4.49	223.1	4.26
	274.4[a]	3.71		
	280.1	3.73	289.7	3.81
	287.5[a]	3.67	295.3[a]	3.76
8.0	220.7	4.49	223.1	4.26
	274.0[a]	3.71		
	280.1	3.74	289.8	3.81
	287.4[a]	3.67	295.0[a]	3.76
9.0	220.7	4.49	223.1	4.27
	274.0[a]	3.70		
	280.0	3.73	289.7	3.81
	287.4[a]	3.66	294.9[a]	3.77
10.0	220.8	4.48	223.0	4.27
	274.2[a]	3.70		
	280.0	3.72	290.0	3.81
	287.5[a]	3.65	295.0[a]	3.77
12.0	220.8	4.48	223.0	4.26
	274.3[a]	3.69		
	279.9	3.72	289.8	3.81
	287.3[a]	3.65	294.8[a]	3.76

[a] shoulder.

additional dissociation-induced spectral changes are not expected in the pH range in which most biochemical reactions occur.

The quantum mechanical interpretation of the absorption spectra of indole derivatives continues to be a challenge [14] (and reference quoted therein). Attention has primarily been focused on the 250–330-nm region which contains two absorption bands with overlapping vibronic lines corresponding to the $^1L_a \leftarrow {}^1A$ and $^1L_b \leftarrow {}^1A$ transitions, for which the short-hand notations, '^1L_a band' and '^1L_b band', are adopted in the text to follow. The influence of solvent effects on their relative positions has been studied in cold expansion jets, comparing the fluorescence excitation spectra of simple model compounds (indole-3-acetic acids themselves decompose under the respective experimental conditions [29]) and their solvent complexes. For 3-methylindole, which contains the basic chromophore of **1**, the lowest energy transition in the gas phase and in extremely non-polar solvents (e.g. solid argon) corresponds to the ^1L_b band [30]. Its position is barely affected when the proton affinity of the solvent increases, while the ^1L_a band experiences a substantial red shift. In the solvents used in this study (ethanol and water), a combined absorbance band with ^1L_a–^1L_b coupling results [31]. As a 3-methyl group has almost the same effect on the indole ring as a 3-CH_2COOH moiety, it may be assumed that the absorbance in the 250–330-nm region in the absorption spectra of **1** and its ring-substituted derivatives has the same combined character. The interpretation of the lower-wavelength maxima appears to be more straightforward. The absorbance at 200–208 nm has been assigned to the ^1B_a band, the peak at 218–232 nm to the ^1B_b band [32].

The influence of ring-substituents differs for the individual absorbance maxima. Red shifts with respect to unsubstituted **1** are more common than blue shifts which are mostly restricted to ring-fluorinated derivatives. The wave numbers for the peak of the ^1B_b band (values for ethanol solutions which afford somewhat sharper peaks) show a satisfactory linear free-energy correlation (Fig. 4; $r = 0.8$, significant at the 0.1% level) with Hammett's σ-constants [33], employing σ_{para} for 5- and 6-substituents and σ_{meta} for 4- and 7-substituents, in analogy to an approach used to rationalize substituent effects on the acidity of the indole NH which is determined by the electron density at the nitrogen atom [34]. Because of the symmetry of the indole nucleus, the same set of σ-constants also describes the electron density at C-3, which appears more relevant in the present case, because the transition moment for the ^1B_b transition calculated for **1** [32] is collinear with a line connecting C-3 and a point around the middle of the C-6—C-7 bond. The above correlation could thus indicate that the ^1B_b transition involves redistribution of electron density localized, in the ground state, primarily at C-3 and likely, to some extent, at the indole nitrogen, which is formally conjugated to C-3 by the interspaced C-3═C-2—N bond system. As a notable exception, the ring-fluorinated indole-3-acetic acids studied here do not fit the correlation shown in Fig. 4. Fluorine has specific resonance effects [35] and may thus interfere with the ^1B_b transition in ways not accessible to the other substituents studied here. Also, the fluorine atoms in 4- and 7-substituted analogues **7** and **23**, the data points of which are particularly distant from the regression line in Fig. 4, are sufficiently close to C-3 and N-1 to affect their electron density by non-bonding interactions, an effect not covered by the Hammett equation. 2-Alkyl derivatives **2**–**4** and aza-analogue **31** were not included in Fig. 4 because the respective σ-constants were not available.

For the remaining absorbance maxima, no convincing correlations with Hammett's σ-constants were found. For the 250–330-nm region, this is most likely due to the fact that the absorbance maxima observed correspond, for different compounds, to different combinations of vibronic lines of the ^1L_a and ^1L_b transitions. For ring-substituted

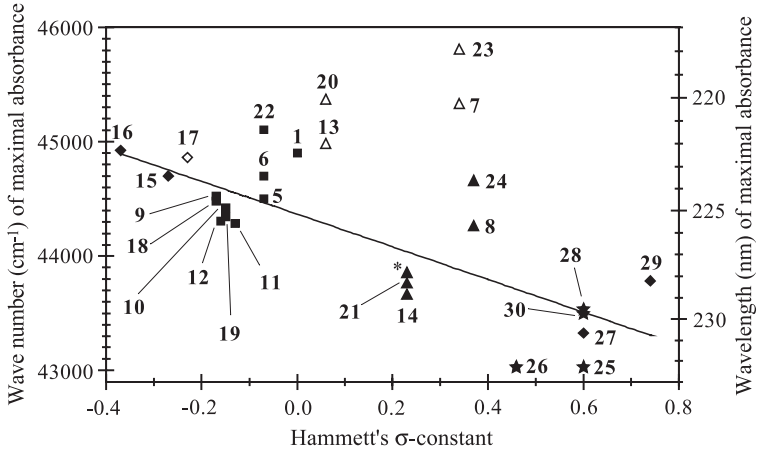

Fig. 4. Correlation between Hammet's σ-constant and the wave numbers of maximal absorbance ($\tilde{N}_{max}$) for the ^1B_b band. The data points are presented by the following symbols to show differences in plant-growth promoting (auxin) activity: black diamonds, weak auxins; plain diamond, **17**, presumed to be a weak auxin on structural grounds, but too water-insoluble for testing in standard bioassays; squares, auxin activity about the same as for **1**; triangles, strong auxins; stars, very strong auxins. The data point marked with an asterisk corresponds to 5-chloroindole-3-acetic acid, using a value taken from Ref. [47] because the compound itself was not available. The regression line [$\tilde{N}_{max} = (-1430 \pm 230) \times \sigma + (44370 \pm 80)$, $r = 0.80$ ($p > 0.999$), standard deviation of data points with respect to regression = 375, $n = 24$] covers all data points except those of ring fluorinated analogues **7**, **13**, **20** and **23** (plain triangles).

indoles, more satisfactory correlations for the absorbance maxima in this spectral region were claimed [36,37], but the range of substituents considered was smaller.

3.2. Fluorescence spectroscopy

Compound **1** has long been known to exhibit fluorescence; its ring-substituted derivatives (out of the set of compounds we examined for UV absorbance), which share this property are listed in Table 3. All alkyl, hydroxy and alkoxy derivatives are included but, among the halogen-substituted analogues, only **13** and **20** were found to be fluorescent at 25 °C, within the sensitivity limits of the experimental setup. The excitation maxima generally occur at 278–280 nm, except for **31** with an excitation maximum of 290 nm. The emission spectra of **1** and **20** are shown as examples, in Fig. 5. As the fluorescence of indole derivatives is known to be pH-dependent [38] (and references quoted therein), the changes in the emission spectrum of **1** were monitored in buffered aqueous solutions covering the pH range of 0–14. The excitation maximum at 280 nm is not pH-dependent, within the limits of experimental error, but differs to some extent from previously reported values, such as 285 [38] and 292 nm [28]. The emission maximum moves from about 360 nm, at pH 2–4, to about 367 nm, at pH 5–8, a shift which has been attributed to the conversion of the undissociated acid ($pK_a = 4.75$ [26]) to the carboxylate ion [28]. The variations in fluorescence quantum

Table 3
Wavelengths of maximal excitation (λ_{exc}), maximal fluorescence emission (λ_f) and fluorescence quantum yields (Q) for indole-3-acetic acid and its ring-substituted derivatives determined in aqueous buffer (refer to Section 2.1 for details)

Compound	pH 7.2			pH 5.0	
	λ_{exc} (nm)	λ_f (nm)	Q	λ_f (nm)	Q
1	280	367	0.33	366	0.30
2	278	370	0.16	367	0.12
3	278	370	0.19	370	0.16
4	278	369	0.20	368	0.16
5	278	355	0.04	352	0.04
6	278	356	0.05	354	0.05
9	276	368	0.22	365	0.20
10	278	369	0.21	364	0.19
11	278	368	0.21	366	0.17
12	278	369	0.20	367	0.17
13	278	368	0.26	367	0.27
15	276	363	0.26	356	0.23
16	278	352	0.19	347	0.13
17	278	366	0.03	358	0.02
18	278	370	0.14	368	0.12
19	278	368	0.16	367	0.13
20	276	372	0.53	371	0.45
22	278	356	0.07	358	0.06
31	290	411	0.01	411	0.01

λ_f and Q were obtained from corrected emission spectra. λ_{exc} was not significantly different at pH 5.0 and 7.2.

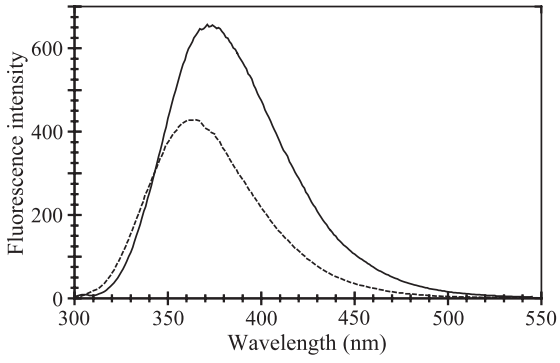

Fig. 5. Fluorescence emission spectra of equimolar solutions ($c = 1.000 \times 10^{-6}$ mol dm^{-3}) of **1** (broken line) and **20** (full line) in aqueous buffer, pH 5.0.

yields (Q) are shown in Fig. 6. While there is no fluorescence at pH ≈ 0, its intensity rapidly increases with increasing pH, to reach a plateau extending from pH 6 to 11. The increase of the slope of the ascending curve around the pK_a value of **1** suggests that the carboxylate ion is more fluorescent than the undissociated acid. The steep decrease of fluorescence above pH 11 appears to be due to quenching by excited state deprotonation of the indole nitrogen [39]. Essentially the same pH-dependence of fluorescence intensities (details not shown) was also found for eight ring-substituted indole-3-acetic acids (**2**, **5**, **13**, **15**, **16**, **18**, **20**, **22**), which represent the structural types studied in this work. The excitation maxima remained within ±2 nm of the values presented in Table 3. The red shifts of the emission maximum due to ionization of the carboxyl group were about the same as for **1**.

In Table 3, the fluorescence data for **1** and its ring-substituted derivatives are compared, based on measurements performed at pH 7.2 and 5.0, to cover the approximate acidity range of the cell compartments in which auxins reside and act in plant and animal systems. As substitution at the indole nucleus should not have major effects on the acidity of the carboxyl group, the latter should, in all compounds shown, be more than 50% dissociated at pH 5 and completely ionized at pH 7.2, and the position of the emission maxima should only move to a minor extent. For **1**, Table 3 shows fluorescence maxima at 366 nm, at pH 5, and at essentially the same wavelength (367 nm), at pH 7.2, in accordance with the value (365 nm) reported by Burnett and Audus [38] (aqueous solution, pH 7.0), but somewhat above the values given by Bridges and Williams [28] (356 nm for the undissociated form and 359 nm for the carboxylate ion). Significant blue shifts, relative to the parent compound, were observed for the 4- and 7-substituted derivatives examined, as well as for **15**–**17**. The fluorescence maxima of most other compounds do not deviate from that of **1** by more than the bandwidth (5 nm) of the emission monochromator, a difference that is not necessarily significant. Ring-methylated indole-3-acetic acids emit at a wavelength about 20 nm above that of the corresponding indoles [24], except for methylation at the 2-position in which case the difference is closer to 10 nm. Depending on the kind and position of the substituent(s), ring-substituted indoles fluoresce from the ^1L_a or the ^1L_b levels, or from a combination of the two [40]. A similar situation may reasonably be assumed for ring-substituted indole-3-acetic acids. The influence of substitution patterns on the position of the emission maximum is thus difficult to interpret.

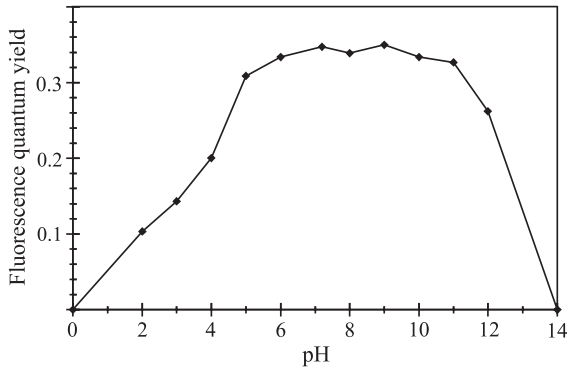

Fig. 6. pH dependence of the fluorescence quantum yield of **1**, as determined in aqueous buffer (refer to Section 2.1 for details).

Compound **1** and its ring-substituted derivatives may also be excited in the region of the ^1B_b band. This implies internal conversion to the ^1L_a and/or ^1L_b levels (depending on the compound considered) from which fluorescence originates, because the emission maxima are at the same positions as in the case of excitation in the 276–280-nm region (data not shown).

The quantum yields listed, in Table 3, for **1** (0.30–0.33) differ substantially from the, frequently quoted [41], value (0.565) reported by Bridges and Williams [28] for the indole-3-acetate ion, but is in excellent accord with the value (0.33) given by Kirby and Steiner [42]. The quantum yield we find for **15** (0.26) also agrees with the literature value of 0.23 (**15** in 0.01 M Tris–HCl, pH 7.4) [43]. Out of the indole-3-acetic acid derivatives examined, the quantum yield of 6-fluoro-analogue **20** exceeds that of the parent compound by 50–60% (Fig. 5). The quantum yield of positional isomer **13** (0.26–0.27), on the other hand, is somewhat less than that of **1** and thus in the same range as for most other ring-substituted derivatives. Much smaller quantum yields (0.03–0.07) were observed for the 4- and 7-alkyl derivatives **5**, **6** and **22** and for **17**. These effects appear to be due to mechanisms involving the indole nucleus, because ring-methylated indoles [24] and 5-methoxyindole [44] have about the same quantum yields as the corresponding indole-3-acetic acids. There is no lack of hypotheses trying to explain why some indole derivatives fluoresce more than others, but little confirming experimental evidence. For instance, the low quantum yield for 5-benzyloxyindole (the chromophore of **17**), at room temperature, appears to be due to the fact that a large part of the absorbed light energy is dissipated through vibration-rotation of the large ring-substituent, because cooling to −196 °C drastically increases fluorescence [28]. 4-Fluorotryptophan, which also fluoresces intensely at that low temperature, stops emitting when warming up to room temperature, in this case (at least in part) because of temperature-dependent chemical reactions involving the excited state [45]. For the protected derivative, *N*-formyl-4-fluorotryptophan methyl ester, UV irradiation in methanol solution was shown to cause photoinduced F/OCH_3 exchange [46]. 4-Fluorinated auxin **7** may be expected to be subject to similar photochemical reactions in its indole moiety. UV irradiation of the methyl ester of 4-chlorinated analogue **8** in methanol solution resulted in photolysis of the C—Cl bond, thus affording the methyl ester of **1** [46].

3.3. UV absorbance and plant-growth promoting activity

Of the indole auxins included in this study, we previously compared the biological activity of **1**, ring-alkylated analogues **2**–**6**, **9**–**12**, **18**, **19** and **22** [20,21], and dichlorinated derivatives **25**–**30** [18], using the same version of the *Avena* coleoptile-section straight-growth bioassay. Fluorinated analogues **7**, **13**, **20** and **23** were tested under closely corresponding conditions [47]. For the remaining compounds, growth-promoting activity has been extensively studied by other authors (e.g. Refs. [2,48–54]), with the only exception of **17** that is not sufficiently water-soluble. An important parameter characterizing the dose–response curves is the half-optimal concentration ($c_{0.5}$), which is believed to reflect the affinity to the, so far hypothetic, receptor(s) involved in the auxin response [52]. When ranked by $c_{0.5}$, the relative growth-promoting activities of ring-substituted indole-3-acetic acids tend to be similar in standard bioassays (for a notable exception, see Ref. [5]), even though the individual values of $c_{0.5}$ are very sensitive to the experimental set-up. In the version of the *Avena* straight growth test we use [18,20,21], 'weak auxins' have $c_{0.5} > 1 \times 10^{-5}$ mol dm^{-3}, auxins with $c_{0.5} = 1 \times 10^{-5}$ to 5×10^{-6} mol dm^{-3} are 'about as strong as **1**', 'strong auxins' are characterized by $c_{0.5} = 5 \times 10^{-6}$ to 1×10^{-6} mol dm^{-3}, and 'very strong auxins' by $c_{0.5} < 1 \times 10^{-6}$ mol dm^{-3}.

The relationship between the absorption maximum for the ^1B_b band and plant-growth promoting activity of ring-substituted indole-3-acetic acids is incorporated in Fig. 4. For the weakest auxins, the respective absorption maximum is at the shortest wavelengths. The larger the red shift for the ^1B_b band, and the larger Hammett's σ-constant for the respective substituent, the stronger the auxin. Only **27** and **29** are weaker auxins than would be predicted from their large red shifts, but this appears to be due to sterical problems in the auxin receptor site(s) [52], not to electronic properties that reflect on their UV-spectra.

Increasing values in the set of Hammett-constants used here mean decreasing electron density at C-3 and the indole nitrogen. The latter was estimated by Porter and Thimann [50] from N–H stretching frequencies in IR spectra and correlated to increasing plant-growth promoting activity, in the context of a more general theory on structure–activity relations for auxins [1] which did not meet with general acceptance. The distribution of strong and weak auxins in Fig. 4 suggests, however, that there is at least some truth to that concept. Ring-substituents may shift UV absorption bands by affecting the electron distribution in the ground state, the excited state, or both. For the position of the ^1B_b band of most ring-substituted indole-3-acetic acids, ground state effects appear to prevail; otherwise a correlation with plant-growth promoting activity (exerted by auxin molecules in their ground-state) would be highly unlikely. The red shift, or decrease in transition energy, we observe for strong auxins would then mean that the respective ring-substituents move electron density in the ground state to positions closer to its localization in the ^1B_b excited state, i.e., with respect to the direction of the transition moment for the ^1B_b-transition [32], to the benzene moiety which carries the substituents.

An increase of electron density in the benzene moiety could lead to stronger interaction with protein bound cations (arginine and lysine residues, metal ions as cofactors) [55] and the residues of aromatic amino acids (Trp, Phe, Tyr) in polypeptides participating in auxin perception while the simultaneous decrease of electron density in the pyrrole moiety could facilitate interaction with electron-rich sites, such as the carboxylate groups of monoamino dicarboxylic acids (Asp, Glu). The type of binding interactions, which occur under real-life conditions, requires further study. In the X-ray structure of ABP1, an auxin-binding plant protein with essential physiological functions [56], co-crystallized with the synthetic auxin, naphthalene-1-acetic acid [57], the face of the ligand's aromatic ring system interacts with the 'edge' of the perpendicularly oriented indole ring of Trp^{151} which flanks the active site.

4. Concluding remarks

It is not unexpected that the absorption and fluorescence spectra of **1** and its ring-substituted derivatives show many similarities to one another and to non-acidic indoles with a similar range of ring-substituents. In many cases, however, the fingerprint pattern in the $^1L_a/^1L_b$ region is sufficiently specific to aid in the identification of unknown indolic auxins. The differences in the position of the, sharper and more intense, ^1B_b band should also permit quantification of the components of binary mixtures of at least some indole auxins, an analytical task likely to arise in substrate competition experiments with physiologically, or biomedically, important auxin-binding proteins. The relationship of the position of the ^1B_b absorbance band and plant-growth promoting activity, albeit only semi-quantitative, affords an independent confirmation of a plausible, but much disputed, hypothesis according to which charge patterns in the aromatic ring system are important for auxin recognition by plant response-mediating proteins, a concept which can almost certainly be extended to auxin-recognizing molecules in human and animal systems [8–10].

The fluorescence of indole auxins, apart from straightforward analytical applications, provides a tool for studying the mechanism of their interaction with auxin-binding proteins. For the most common natural auxin, **1**, the fluorescence maximum and quantum yield in aqueous solutions of physiological pH, are about the same as the respective parameters for tryptophan, a circumstance that makes it difficult to assign the mutual changes which occur when the amino acid becomes part of a protein to which **1** binds as a ligand. Exchanging the tryptophan(s) in a peptide chain by a non-fluorescent analogue, such as 4-fluorotryptophan [58,59], would permit undisturbed observation

of the fluorescence of **1**. Another possibility would be replacing tryptophan by its 7-aza-analogue which has its excitation and emission maxima to the red of **1** while emission wavelength and quantum yield are particularly sensitive to local environmental effects, a property which is, with increasing success, exploited in studies on protein-ligand interactions and other aspects of protein structure and dynamics [58–60]. If modification of the auxin-binding protein is not feasible, it may be worth considering ligand binding studies using 7-aza-analogue **31** instead of natural auxin **1**. As a 7-azaindole derivative, **31** should show similar useful photophysical properties as 7-aza-tryptophan. In particular, **31** responds to excitation at higher wavelengths than the tryptophan residues in an auxin-binding protein. In solution, the auxin analogue fluoresces about 40 nm to the red with respect to Trp, and at least part of this difference is likely to persist in a protein environment. The quantum yield of **31** is expected to increase substantially when the compound passes from aqueous solution into a hydrophobic binding site. Another auxin analogue worth testing as a ligand would be **20**, which may well be distinguishable from tryptophan residues by the intensity of its fluorescence (quantum yield in solution 50–60% larger than for **1**), unless entering the auxin-binding site causes exceptionally severe quenching effects. If substrate-induced conformational changes of an auxin-binding protein are of primary interest, using a non-fluorescent auxin as a ligand should permit undisturbed observation of the fluorescence of the tryptophan residues. Comparison of Table 3 and Fig. 4 reveals 10 strong and 2 weak (**27**, **29**) auxins, which should be suitable for such experiments.

Acknowledgements

Supported by grants no. 0098037 (M.K., G.P.), 0098080 (V.M.), 0119620 (V.T.), 0119641 (N.G.) and 0178067 (D.C., M.Š.), awarded by the Ministry of Science and Technology of the Republic of Croatia.

References

[1] K.V. Thimann, Hormone Action in the Whole Life of Plants, The University of Massachusetts Press, Amherst, 1977.
[2] Å. Jönsson, Chemical structure of auxins and antiauxins, in: W. Ruhland (Ed.), Encyclopedia of Plant Physiology, vol. 14, Springer Verlag, Berlin, 1961, pp. 959–1006.
[3] J.-C. Gandar, C. Nitsch, Isolement de l'ester méthylique d'un acide chloro-3-indolylacétique à partir de graines immatures de Pois, *Pisum sativum* L, C. R. Acad. Sci. (Paris), Sér. D 265 (1967) 1795–1798.
[4] S. Marumo, H. Hattori, H. Abe, K. Munakata, Isolation of 4-chloroindolyl-3-acetic acid from immature seeds of *Pisum sativum*, Nature 219 (1968) 959–960.
[5] D.M. Reinecke, 4-Chloroindole-3-acetic acid and plant growth, Plant Growth Regul. 27 (1999) 3–13.
[6] O. Salcher, F. Lingens, Biosynthese von Pyrrolnitrin. Nachweis von 3-Chloranthranilsäure und 7-Chlorindolessigsäure im Kulturmedium von *Pseudomonas aureofaciens*, Tetrahedron Lett. 34 (1978) 3101–3102.
[7] C. Lübbe, K.-H. van Pée, O. Salcher, F. Lingens, The metabolism of tryptophan and 7-chlorotryptophan in *Pseudomonas pyrrocinia* and *Pseudomonas aureofaciens*, Hoppe-Seyler's Z. Physiol. Chem. 364 (1983) 447–453.
[8] A. Bertuzzi, G. Mingrone, A. Gandolfi, A.V. Greco, S. Ringoir, R. Vanholder, Binding of indole-3-acetic acid to human serum albumin and competition with l-tryptophan, Clin. Chim. Acta 265 (1997) 183–192.
[9] A.V. Greco, G. Mingrone, A. Favuzzi, A. Bertuzzi, A. Gandolfi, R. DeSmet, R. Vanholder, G. Gasparrini, Subclinical hepatic encephalopathy: role of tryptophan binding to albumin and the competition with indole-3-acetic acid, J. Investig. Med. 48 (2000) 274–280.
[10] M. Motojima, A. Hosokawa, H. Yamato, T. Muraki, T. Yoshioka, Uraemic toxins induce proximal tubular injury via organic anion transporter 1-mediated uptake, Br. J. Pharmacol. 135 (2002) 555–563.
[11] L.K. Folkes, P. Wardman, Oxidative activation of indole-3-acetic acids to cytotoxic species—a potential new role for plant auxins in cancer therapy, Biochem. Pharmacol. 61 (2001) 129–136.
[12] L.K. Folkes, P. Wardman, Enhancing the efficacy of photodynamic cancer therapy by radicals from plant auxin (indole-3-acetic acid), Cancer Res. 63 (2003) 776–779.
[13] S. Rossiter, L.K. Folkes, P. Wardman, Halogenated indole-3-acetic acids as oxidatively activated prodrugs with potential for targeted cancer therapy, Bioorg. Med. Chem. Lett. 12 (2002) 2523–2526.
[14] P.R. Callis, ^{1}La and ^{1}Lb transitions of tryptophan: applications of theory and experimental observations to fluorescence of proteins, Methods Enzymol. 278 (1997) 113–150.
[15] M.M. Robison, B.L. Robison, 7-Azaindole: I. Synthesis and conversion to 7-azatryptophan and other derivatives, J. Am. Chem. Soc. 77 (1955) 457–460.
[16] M.M. Robison, B.L. Robison, 7-Azaindole: III. Syntheses of 7-aza analogs of some biologically significant indole derivatives, J. Am. Chem. Soc. 78 (1956) 1247–1251.
[17] K.C. Engvild, Preparation of chlorinated 3-indolylacetic acids, Acta Chem. Scand., Sect. B 31 (1977) 338–339.
[18] S. Antolić, B. Salopek, B. Kojić-Prodić, V. Magnus, J.D. Cohen, Structural characterization and auxin properties of dichlorinated indole-3-acetic acids, Plant Growth Regul. 27 (1999) 21–31.
[19] D.M. Reinecke, J.A. Ozga, V. Magnus, Effect of halogen substitution of indole-3-acetic acid on biological activity in pea fruit, Phytochemistry 40 (1995) 1361–1366.
[20] B. Nigović, S. Antolić, B. Kojić-Prodić, R. Kiralj, V. Magnus, B. Salopek-Sondi, Correlation of structural and physico-chemical parameters with the bioactivity of alkylated derivatives of indole-3-acetic acid, a phytohormone (auxin), Acta Crystallogr., B Struct. Sci. 56 (2000) 94–111.
[21] S. Antolić, E. Dolušić, E.K. Kožić, B. Kojić-Prodić, V. Magnus, M. Ramek, S. Tomić, Auxin activity and molecular structure of 2-alkylindole-3-acetic acids, Plant Growth Regul. 39 (2003) 235–252.
[22] J.N. Miller, Standards for Fluorescence Spectrometry, Chapman and Hall, London, 1981.
[23] R.F. Chen, Fluorescence quantum yields of tryptophan and tyrosine, Anal. Lett. 1 (1967) 35–42.
[24] M.R. Eftink, Y. Jia, D. Hu, C.A. Ghiron, Fluorescence studies with tryptophan analogues: excited state interactions involving the side chain amino group, J. Phys. Chem. 99 (1995) 5713–5723.
[25] D.H. Williams, I. Fleming, Spectroscopic Methods in Organic Chemistry, McGraw-Hill Publishing, Maidenhead, 1966.
[26] S. Budavari (Ed.), The Merck Index, 11th ed., Merck, Rahway, NJ, USA, 1989, p. 4869.
[27] Y. Chen, R.L. Rich, F. Gal, J.W. Petrich, Fluorescent species of 7-azaindole and 7-azatryptophan in water, J. Phys. Chem. 97 (1993) 1770–1780.

[28] J.W. Bridges, R.T. Williams, The fluorescence of indoles and aniline derivatives, Biochem. J. 107 (1968) 225–237.
[29] R. Bersohn, U. Even, J. Jortner, Fluorescence excitation spectra of indole, 3-methyl indole, and 3-indole acetic acid in supersonic jets, J. Chem. Phys. 80 (1984) 1050–1058.
[30] B. Fender, P.R. Callis, ^1L_a origin locations of methylindoles in argon matrices, Chem. Phys. Lett. 262 (1996) 343–348.
[31] K.W. Short, P.R. Callis, Evidence for ^{1}La fluorescence from jet-cooled 3-methylindole-polar solvent complexes, J. Chem. Phys. 113 (2000) 5235–5244.
[32] F. Tomas-Vert, C.A. Ponce, M.R. Estrada, J. Silber, J. Singh, J. Anunciatta, Experimental and theoretical studies on the electronic spectra of indole-3-acetic acid and its anionic and protonated species, J. Mol. Struct. 246 (1991) 203–215.
[33] C. Hansch, A. Leo, D. Hoekman, Exploring QSAR: hydrophobic, electronic and steric constants, ACS Professional Reference Book, vol. 2, American Chemical Society Publishers, Columbus, OH, 1995.
[34] M.A. Muñoz, P. Guardado, J. Hidalgo, C. Carmona, M. Balón, An experimental and theoretical study of the acid–base properties of substituted indoles, Tetrahedron 48 (1992) 5901–5914.
[35] E.L. Wehry, L.B. Rogers, Application of linear free energy relations to electronically excited states of monosubstituted phenols, J. Am. Chem. Soc. 87 (1965) 4234–4238.
[36] A. Tine, J.-J. Aaron, Quantitative treatment of the substituent effects on the electronic absorption spectra of indole derivatives, Spectrochim. Acta, Part A: Mol. Biomol. Spectrosc. 52 (1996) 69–70.
[37] J.-J. Aaron, A. Tine, C. Villiers, C. Párkányi, D. Bouin, Electronic absorption and fluorescence spectra of indole derivatives. Quantitative treatment of the substituent effects and a theoretical study, Croat. Chem. Acta 56 (1983) 157–168.
[38] D. Burnett, L.J. Audus, The use of fluorimetry in the estimation of naturally-occurring indoles in plants, Phytochemistry 3 (1964) 395–415.
[39] E. vander Donckt, Fluorescence solvent shifts and singlet excited state p*K*'s of indole derivatives, Bull. Soc. Chim. Belg. 78 (1969) 69–75.
[40] M.R. Eftink, L.A. Selvidge, P.R. Callis, A.A. Rehms, Photophysics of indole derivatives: experimental resolution of L_a and L_b transitions and comparison with theory, J. Phys. Chem. 94 (1990) 3469–3479.
[41] W.A. Remers, Properties and reactions of indoles, in: W.J. Houlihan (Ed.), Indoles, Part One, Wiley, New York, 1972, pp. 1–226.
[42] E.P. Kirby, R.F. Steiner, The influence of solvent and temperature upon the fluorescence of indole derivatives, J. Phys. Chem. 74 (1970) 4480–4490.
[43] R.F. Chen, Fluorescence of protonated excited-state forms of 5-hydroxytryptamine (serotonin) and related indoles, Biochemistry 60 (1968) 598–605.
[44] M.V. Hershberger, R.W. Lumry, The photophysics of 5-methoxyindole. A non-exciplex forming indole: additional evidence for two classes of exciplexes, Photochem. Photobiol. 23 (1976) 391–397.
[45] J.L. Hott, R.F. Borkman, The non-fluorescence of 4-fluorotryptophan, Biochem. J. 264 (1989) 297–299.
[46] N.-C.C. Yang, A. Huang, D.-D.H. Yang, Photodehalogenation of 4-haloindoles, J. Am. Chem. Soc. 111 (1989) 8060–8061.
[47] S. Antolić, B. Kojić-Prodić, S. Tomić, B. Nigović, V. Magnus, J.D. Cohen, Structural studies on monofluorinated derivatives of the phytohormone indole-3-acetic acid (auxin), Acta Crystallogr., Sect. B 52 (1996) 651–661.
[48] S.P. Findlay, G. Dougherty, The activity of certain substituted indoleacetic acids as plant hormones in the pea test, J. Biol. Chem. 183 (1950) 361–364.
[49] K.V. Thimann, Auxin activity of some indole derivatives, Plant Physiol. 33 (1958) 311–321.
[50] W.L. Porter, K.V. Thimann, Molecular requirements for auxin action: I. Halogenated indoles and indoleacetic acid, Phytochemistry 4 (1965) 229–243.
[51] M. Böttger, K.C. Engvild, H. Soll, Growth of *Avena coleoptiles* and pH drop of protoplast suspensions induced by chlorinated indoleacetic acids, Planta 140 (1978) 89–92.
[52] G.F. Katekar, Auxins: on the nature of the receptor site and molecular requirements for auxin activity, Phytochemistry 18 (1979) 223–233.
[53] G.F. Katekar, A.E. Geissler, Auxins: II. The effect of chlorinated indolylacetic acids on pea stems, Phytochemistry 21 (1982) 257–260.
[54] G.F. Katekar, A.E. Geissler, Structure–activity differences between indoleacetic acid auxins on pea and wheat, Phytochemistry 22 (1983) 27–31.
[55] N. Zacharias, D.A. Dougherty, Cation–π interactions in ligand recognition and catalysis, Trends Pharmacol. Sci. 23 (2002) 281–287.
[56] R.M. Napier, K.M. David, C. Perrot-Rechenmann, A short history of auxin-binding proteins, Plant Mol. Biol. 49 (2002) 339–348.
[57] E.-J. Woo, J. Marshall, J. Bauly, J.-G. Chen, M. Venis, R.M. Napier, R.W. Pickersgill, Crystal structure of auxin-binding protein 1 in complex with auxin, EMBO J. 21 (2002) 2877–2885.
[58] J.B.A. Ross, A.G. Szabo, C.W.V. Hogue, Enhancement of protein spectra with tryptophan analogs: fluorescence spectroscopy of protein–protein and protein–nucleic acid interactions, Methods Enzymol. 278 (1997) 151–190.
[59] S.M. Twine, A.G. Szabo, Fluorescent amino acid analogues, Methods Enzymol. 360 (2004) 104–127.
[60] V. de Filippis, S. de Boni, E. de Dea, D. Dalzoppo, C. Grandi, A. Fontana, Incorporation of the fluorescent amino acid 7-azatryptophan into the core domain 1–47 of hirudin as a probe of hirudin folding and thrombin recognition, Protein Sci. 13 (2004) 1489–1502.